Si-Al ordering in leucite group minerals and ion-exchanged analogues: An MAS NMR study

SIMON C. KOHN,[1,]* C. MICHAEL B. HENDERSON,[2] AND RAY DUPREE[1]

[1]Department of Physics, University of Warwick, Coventry, CV4 7AL, U.K.
[2]Department of Earth Sciences, University of Manchester, Manchester, M13 9PL, U.K.

ABSTRACT

Two series of leucite group materials, with K, Rb, and Cs as extra-framework cations, have been synthesized by ion exchange from a natural well-ordered analcite and a natural disordered leucite. ^{29}Si and ^{27}Al MAS NMR data for the analcite-derived series provide complementary information on tetrahedral cation ordering. The ordering in terms of the number of Al next-nearest neighbors, $Q^4(nAl)$ (short-range order), does not change significantly during ion exchange, indicating that Al and Si remain essentially fixed in their original positions. In contrast, the ordering of Al over T1, T2, and T3 (long-range order) for the analcite-derived series changes dramatically with changing alkali cation; the Al occupancies for the three analcite-derived samples expressed as T1:T2:T3 are approximately 0.25:0.50:0.25 for $KAlSi_2O_6$, 0.40:0.20:0.40 for $RbAlSi_2O_6$, and 0.15:0.70:0.15 for $CsAlSi_2O_6$. During the ion exchange, at temperatures above the cubic-tetragonal phase transitions, only one symmetrically distinct T site is present. It is proposed that on cooling through the cubic-tetragonal phase transition the structure collapses around the non-framework cations to give the lowest energy Si-Al distribution over the three T sites irrespective of the original T-site ordering in the starting material. Our data suggest that the identity of the cation in the W site affects the orientation of the framework distortions associated with the cubic-tetragonal phase transition and leads to the possibility that a particular tetrahedral cation site can take on the characteristics of a T1, T2, or T3 site. The data and their interpretation have important implications for the mechanism of this type of structural phase transition.

INTRODUCTION

There has recently been considerable interest in the ordering behavior and structural phase transitions in leucite group minerals. As well as studies of natural $KAlSi_2O_6$ leucite (e.g., Phillips et al. 1989; Hatch et al. 1990; Ito et al. 1991; Kohn et al. 1995; Baltisberger et al. 1996) there have been studies of leucite samples with Rb or Cs replacing K (Phillips and Kirkpatrick 1994; Palmer et al. 1997), leucite with Fe^{3+} replacing Al (e.g., Lange et al. 1986; Bell and Henderson 1994), and examples with divalent cations, such as Mg, Zn, Cd, Ni, and Mn, replacing Al (Kohn et al. 1991, 1994; Bell et al. 1994a, 1994b; Bell and Henderson 1996).

Kohn et al. (1995) studied the Si-Al ordering in two contrasting samples of leucite using MAS NMR. One sample was natural and the other was synthesized by ion exchange from an analcite with a small distribution of Al next-nearest neighbors (NNN). In the ion-exchange-derived specimen, the restricted range of NNN environments enabled a good estimate of the ordering pattern of

Si and Al over the three T sites. The T2 sites contained 45–50% of the Al with the remainder distributed approximately equally between the T1 and T3 sites. It was found that the ^{29}Si spectrum of the natural leucite sample could be fitted with a wide variety of Al distributions including either Al ordering onto T2 or with Al ordering onto T1 and T3. By analogy with the analcite-derived sample, and considering previous neutron and X-ray data, Al ordering onto T2 was preferred over alternative schemes.

The present paper represents an extension of the work of Kohn et al. (1995) in that Rb- and Cs-substituted analogues of the natural leucite and analcite samples were prepared and studied using MAS NMR. The NMR data complement the information on framework geometries recently reported by Palmer et al. (1997), but in addition the changes in short- and long-range order during ion exchanges probed by NMR provide a novel insight into the nature of the cubic-tetragonal phase transition.

EXPERIMENTAL METHODS

Samples

Two natural starting materials were used in this study: analcite M416 from Monteccio, Maggiore, Italy, and leucite from Alban Hills, Italy. These were converted into

* Present address: Department of Geology, University of Bristol, Wills Memorial Building, Queens Road, Bristol, BS8 1RJ, U.K.

TABLE 1. List of samples, ion-exchange conditions, and partial chemical analyses

| Sample | Starting material | Ion exchange | | | Na (ppm) | K (ppm) |
		Salt	T (°C)	Duration		
KAS2	Alban Hills	—	—	—	4600	n.a.
RAS1	Alban Hills	RbCl	770	2 × 6 h	180	1200
CAS4	Alban Hills	CsCl	700	4 × 6 h	500	1.54 wt%
KAS3	Analcite	KCl	850	2 × 3 h	310	n.a.
RAS2	Analcite	RbCl	770	2 × 6 h	64	32
CAS2	Analcite	CsCl	700	2 × 6 h	1340	n.d.

Notes: n.a. = not analyzed; n.d. = none detected.

two series of leucite analogues by ion exchange in KCl, RbCl, or CsCl at temperatures between 700 and 850 °C, then cooled, leached, and thoroughly washed. In all cases the temperature of ion exchange is higher than the tetragonal-cubic phase transition temperature of the product; the transition temperatures are about 660, 480, and 120 °C for the K, Rb, and Cs analogues, respectively (Taylor and Henderson 1968; Palmer et al. 1997). The degree of exchange was checked by powder XRD, and additional exchanges were performed to produce structurally homogeneous products. The final products were partially analyzed by atomic absorption spectroscopy for Na or K depending on the starting material. The ion-exchange conditions and partial chemical analyses of the products are given in Table 1. The spectra for analcite, Alban Hills leucite, and $KAlSi_2O_6$ leucite prepared by ion exchange from analcite were presented by Kohn et al. (1995) and are not discussed again in detail. The spectra nonetheless are included here to facilitate comparison with the Rb and Cs analogues.

NMR

The ^{29}Si NMR data were acquired using a Bruker MSL360 spectrometer operating at 71.535 MHz with MAS at 3.5–4.0 kHz. The analcite-derived series were found to have extremely long $T1$ relaxation times, requiring the use of recycle delays up to 7200 s. The delays made data acquisition very time consuming and results in poor signal-to-noise ratios for some samples.

For ^{27}Al spectra, resolution of the different Al environments required the use of the highest possible field available to us, 14.1 T. Therefore a Varian VXR 600 was used with a home-built probe based on a Doty Scientific spinning assembly capable of MAS up to 14 kHz. No resolved second-order quadrupolar line shapes were observed, and no attempts to extract quadrupolar parameters were made.

RESULTS

^{29}Si MAS NMR

Analcite-derived series. The spectrum for analcite itself (Kohn et al. 1995) consists of a peak at −96.6 ppm due to Q^4(2Al) Si atoms, with small peaks at −91.5 ppm and −102 ppm due to Q^4(3Al) and Q^4(1Al) Si atoms, respectively. A fit of a cross-polarization spectrum of
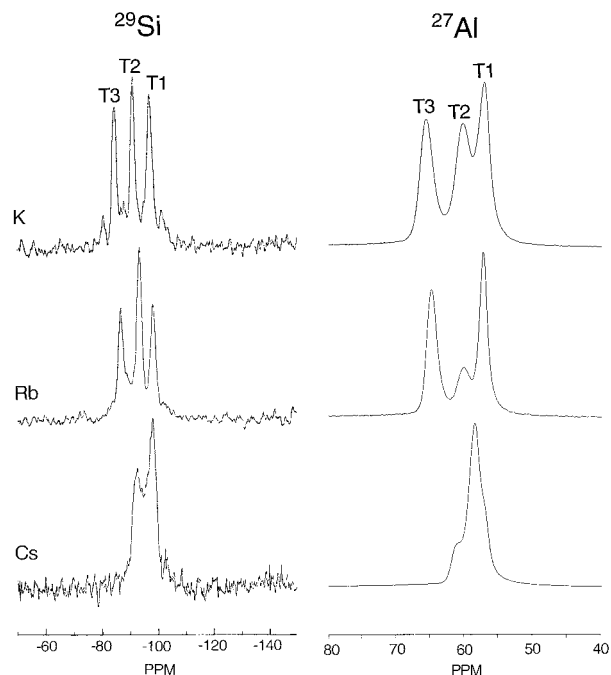

FIGURE 1. MAS NMR spectra for leucite samples synthesized by ion exchange from M416 analcite. The left column displays the ^{29}Si spectra, and the ^{27}Al spectra (14.1 T) are in the right column. (**top**) $KAlSi_2O_6$ (after Kohn et al. 1995); (**center**) $RbAlSi_2O_6$ (^{29}Si spectrum acquired using 215 2 μs pulses, 240 s recycle delay); (**bottom**) $CsAlSi_2O_6$ (^{29}Si spectrum acquired using 48 2 μs pulses, 1 h recycle delay). All ^{27}Al spectra were acquired using 4032 1 μs pulses and a recycle delay between 0.1 and 1 s.

analcite (Kohn et al. 1995) showed that 80% of the Si atoms have two Al NNN, i.e., a smaller distribution of Al NNN than samples studied previously (e.g., Murdoch et al. 1988; Phillips and Kirkpatrick 1994). This provides an excellent opportunity to synthesize leucite samples by ion exchange, with a similarly narrow distribution of Al NNN, and this is the key to the most interesting data presented in this paper.

The ^{29}Si MAS NMR spectrum of $KAlSi_2O_6$ leucite obtained by ion exchange from analcite was reported by Kohn et al. (1995), and is shown in Figure 1. The three main peaks at −97.3, −91.25, and −84.8 ppm are due to Q^4(2Al) Si atoms on three tetrahedral sites, T1, T2, and T3. The spectrum can be simulated in different ways, but the one preferred by Kohn et al. (1995) implies that 72–74% of the Si is in Q^4(2Al) sites, and that the Al occupancies are approximately $g_1 = 0.25$, $g_2 = 0.5$, and $g_3 = 0.25$ [see Kohn et al. (1995) for details and estimates of errors].

The ^{29}Si spectrum of the Rb member of this series is similar to that for the $KAlSi_2O_6$ leucite, but the spectrum is of better quality because of more rapid spin-lattice relaxation (presumably because of dipolar relaxation from the abundant Rb nuclei). As found for the $KAlSi_2O_6$ leucite, the three peaks at −98.2, −93.3, and −86.7 ppm

correspond to Q[4](2Al) Si in T1, T2, and T3 sites, respectively. A major difference, however, is that the T2 peak is clearly more intense than the other two. The small shoulders at about −83 and −102 ppm are probably due to T3(3Al) and T1(1Al) Si, respectively, and are similar in size to the analogous peaks in the $KAlSi_2O_6$ leucite member of this series. The Q[4](nAl) distribution appears therefore to be comparable with that for the $KAlSi_2O_6$ leucite. The other small 3Al and 1Al peaks that are likely to be present are not resolvable from the much larger 2Al peaks (the three main peaks in the spectrum). We do not intend to report rigorous fits for the Rb and Cs series in this paper, but on the basis of a three-peak fit to the spectrum we estimate that 42 ± 2% of the Si is in T2 sites, with 29 ± 4% in each of T1 and T3. This corresponds to T site Si occupancies of 0.58 ± 0.08, 0.84 ± 0.04, and 0.58 ± 0.08 for T1, T2, and T3, respectively. Thus by difference, the Al occupancies are predicted to be g_1 = 0.42 ± 0.08, g_2 = 0.16 ± 0.04, and g_3 = 0.42 ± 0.08.

The appearance of the spectrum for the analcite-derived $CsAlSi_2O_6$ leucite is somewhat different, although since $CsAlSi_2O_6$ leucite is also tetragonal at room temperature (Palmer et al. 1997), three T sites are expected. The spectrum is indeed consistent with the presence of three peaks attributed to T1, T2, and T3 sites, and can be simulated with peaks at −98.9, −96.1, and −92.7, respectively. Q[4](nAl) appears to be consistent with the K and Rb series, but the 1Al and 3Al peaks are so poorly resolved that only a three-peak fit to the spectrum was attempted. The best simulation suggests that the relative areas of the three peaks are 47%, 15%, and 38%. However, the Si/Al ratio of two and the small concentrations of Si with other than two Al NNN constrain the Si occupancies of the T1 and T3 sites to be the same (Kohn et al. 1995). Therefore we take the mean and assume relative concentrations of 42.5 ± 6% in T1 and T3 and 15 ± 4% in T2, giving Al occupancies of g_1 = 0.15 ± 0.12, g_2 = 0.70 ± 0.08, and g_3 = 0.15 ± 0.12. Thus, in marked contrast to the $RbAlSi_2O_6$ leucite, it appears that, as for $KAlSi_2O_6$ leucite, Al is partitioned strongly onto the T2 site (though even more strongly than in $KAlSi_2O_6$).

In addition to the remarkable changes in T-site ordering described above, ^{29}Si MAS NMR also provides information on the intertetrahedral bond angles (T-O-T) and thus the degree of collapse of the framework. If all the [29]Si spectra in Figure 1 are compared, it can be seen that the differences between the peak positions of the three sites become smaller as K is replaced by the larger alkali cations, as would be expected. This is consistent with the reduction in the tetragonal distortion reported by Taylor and Henderson (1968) and Palmer at al. (1997). Compared with $KAlSi_2O_6$ leucite, the Rb analogue has peaks with more negative shifts, i.e., larger T-O-T angles, and for $CsAlSi_2O_6$ leucite the T3 and T2 peaks are at even more negative shifts whereas the T1 peak is only slightly more negative. The change to more negative shifts can be correlated with increasing mean T-O-T angle and increasing T-T distances, and thus to a more expanded
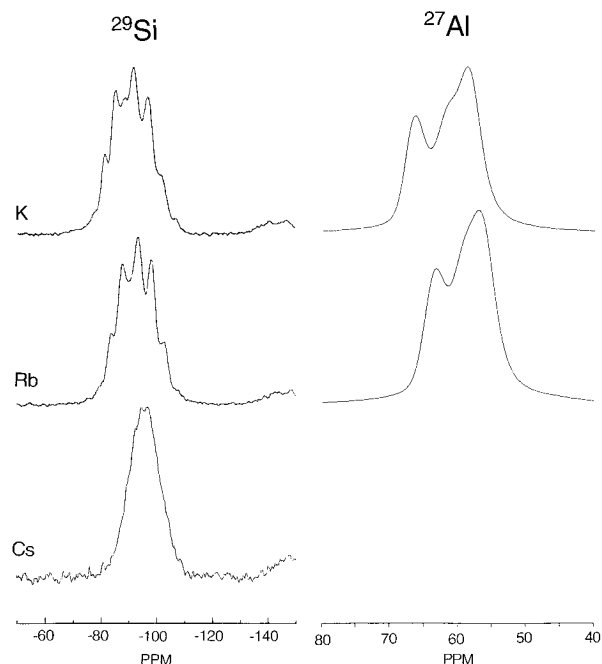

FIGURE 2. MAS NMR spectra for Alban Hills leucite and samples synthesized by ion exchange for which Alban Hills leucite was used as a starting material. The left column displays the [29]Si spectra, and the [27]Al spectra (14.1 T) are in the right column. (**top**) Alban Hills $KAlSi_2O_6$ leucite (after Kohn et al. 1995); (**center**) $RbAlSi_2O_6$ ([29]Si spectrum acquired using 3600 2 μs pulses, 1 s recycle delay); (**bottom**) $CsAlSi_2O_6$ ([29]Si spectrum acquired using 484 2 μs pulses, 120 s recycle delay). [27]Al spectra were acquired using 4032 1 μs pulses and a recycle delay of 0.1 s.

framework for the larger cations. Such changes agree with the data of Palmer et al. (1997).

Alban Hills leucite-derived series. The [29]Si spectrum for natural Alban Hills leucite is given in Figure 2. It consists of a relatively broad resonance with eight discernible narrower features (peaks or shoulders). This spectrum was presented by Kohn et al. (1995), who discussed the fitting in detail. For the purposes of this paper the important points to note are that the three largest peaks are in approximately the same positions as those in the analcite-derived sample, and that for each of the three T sites there is a fairly wide distribution of numbers of Al NNN. Thus, whereas the analcite-derived leucite contains mostly Q[4](2Al) Si, with small numbers of Q[4](3Al) and Q[4](1Al) Si, the natural specimen contains a wider distribution of numbers of Al NNN, i.e., Q[4](4Al) and Q[4](0Al) in addition to Q[4](3Al), Q[4](1Al), and Q[4](2Al). Kohn et al. (1995) used the ordering pattern for analcite-derived $KAlSi_2O_6$ leucite to help in fitting the more complex spectrum of natural Alban Hills leucite. They proposed a model (based largely on comparison with the analcite-derived sample) in which Al is partitioned onto T2 sites with g_1 = 0.25, g_2 = 0.5, and g_3 = 0.25. This scheme is different from those proposed previously (Brown et al. 1987; Murdoch et al. 1988; Phillips et al.

1989), despite the similarity of the spectra in all four studies, and illustrates the difficulty in uniquely fitting a poorly resolved spectrum containing up to 15 contributing peaks.

The spectrum for $RbAlSi_2O_6$ Alban Hills leucite is similar to that of the Alban Hills leucite itself, but the spread of shifts is 1.5 ppm smaller. As for the $KAlSi_2O_6$ leucite samples, the three largest peaks correspond closely in position to the three peaks in the ^{29}Si spectrum of the analcite-derived $RbAlSi_2O_6$.

The ^{29}Si spectrum of the $CsAlSi_2O_6$ from ion exchange of Alban Hills leucite consists of a broad resonance, with no peaks resolved for the individual T sites or Al NNN. The spectrum reported by Phillips and Kirkpatrick (1994) for a $CsAlSi_2O_6$ leucite synthesized by ion exchange from a natural leucite is somewhat different from ours. It does contain some resolved features and the entire envelope covers a smaller shift range. These features probably indicate that the Phillips and Kirkpatrick (1994) sample had a higher degree of exchange than our sample CAS4.

^{27}Al MAS NMR

Analcite-derived series. The ^{27}Al spectrum of analcite consists of a single peak at 57.9 ppm with a FWHM of 2.5 ppm, consistent with the presence of only one tetrahedral site, or possibly more than one very similar site.

The spectrum for KAS3 is particularly interesting as it consists of three clearly resolved sites of approximately equal intensities, attributed to T1, T2, and T3 sites. Kohn et al. (1995) analyzed this spectrum in some detail, but were unable to produce a simulation that agreed well with the results from the ^{29}Si spectrum. They concluded that the ordering deduced from the ^{29}Si spectrum was more reliable because of uncertainties in simulating the spectra for quadrupolar-broadened ^{27}Al spectra.

The most interesting feature of the spectrum for RAS2 is that the intensity of the T2 peak is smaller than that for the T1 and T3 peaks. This incontrovertible evidence for ordering of Al onto T1 and T3 is consistent with the ^{29}Si spectrum that suggested Si is ordered onto T2. Simulations of the ^{27}Al spectrum using peaks with 70% Gaussian and 30% Lorentzian character give values of Al occupancy of $g_1 = 0.41$, $g_2 = 0.18$, and $g_3 = 0.41$. These simulations do not include any quadrupolar contribution to the line shape, and are thus somewhat uncertain, but we judge that the errors in the Al occupancies are unlikely to be greater than ± 0.05. The Al occupancies determined from ^{29}Si NMR are $g_1 = 0.42$, $g_2 = 0.16$, and $g_3 = 0.42$, and the fact that the data from the ^{29}Si and ^{27}Al spectra are in such good agreement lends support to this analysis. Changes also occur in the positions of the peaks in comparison with the K-exchanged sample. The T1 peak is at approximately the same shift as in KAS3, but the T3 peak is shifted to lower frequency by about 1 ppm. The result is that the spread of shifts (and hence T-O-T bond angles) is smaller than in KAS3.

The ^{27}Al spectrum of analcite-derived $CsAlSi_2O_6$ leucite consists of a single asymmetrical peak, with a shoulder on each side. We interpret this as a large T2 peak with small T1 and T3 peaks. Reasonable fits to the spectrum were obtained using a range of parameters, but in all cases the Al occupancy of T2 is greater than 60%. Typical values are $g_1 = 0.16 \pm 0.05$, $g_2 = 0.71 \pm 0.10$, and $g_3 = 0.13 \pm 0.05$, well within error of the values of $g_1 = 0.15 \pm 0.12$, $g_2 = 0.70 \pm 0.08$, and $g_3 = 0.15 \pm 0.05$ obtained from the ^{29}Si spectrum.

Alban Hills leucite-derived series. The ^{27}Al spectra for the Alban Hills leucite derived series are much less well resolved than those for the analcite-derived series. This is probably due to distributions in the quadrupole parameters as well as the isotropic chemical shifts (see Kohn et al. 1995). In the spectrum for KAS2, a small shoulder at about 61.5 ppm due to T2 is visible between the peaks due to T3 and T1 at about 66.5 ppm and 58.5 ppm, respectively, but it would be impossible to extract quantitative site occupancies or isotropic chemical shifts from this spectrum alone.

The spectrum for the Rb derivative is even less well resolved, presumably because of the smaller difference in isotropic shifts between the peaks or larger quadrupole coupling constants. The spectrum for the Cs derivative was not recorded, but it is most unlikely that it contains useful information about Si-Al order, bearing in mind the unresolved nature of the ^{29}Si spectrum for this sample. The spectrum reported by Phillips and Kirkpatrick (1994) for natural leucite-derived $CsAlSi_2O_6$ shows only one broad peak. They commented that T-O-T angle correlations suggest that three peaks should be observed. It is possible that their failure to see three peaks is due to strong Al ordering onto T2 as observed in our sample CAS2.

DISCUSSION

Short-range order vs. long-range Si-Al order

There are two principal types of order-disorder that can be quantified from MAS NMR spectra of leucite-group samples. These are: (1) short-range order reflected in the Al NNN distributions around Si, i.e., n in $Q^4(nAl)$ and (2) long-range ordering of Al over the different tetrahedral sites T1, T2, and T3.

One of the most important observations made from the data in this study is that there appear to be only small changes in the Al NNN distributions during the ion-exchange process. Thus analcite and the leucite samples derived from it all have a small NNN distribution, with about 70–80% of the Si having $Q^4(2Al)$ local environments and 10–15% each in $Q^4(3Al)$ and $Q^4(1Al)$. In contrast, Alban Hills leucite (Kohn et al. 1995) and its $RbAlSi_2O_6$ and $CsAlSi_2O_6$ derivatives (by visual inspection of the ^{29}Si spectra in Fig. 2) each have a wide range of numbers of Al NNN, including $Q^4(0Al)$, $Q^4(1Al)$, $Q^4(2Al)$, $Q^4(3Al)$, and $Q^4(4Al)$. Although the lack of resolution in the spectra precludes unambiguous determination of the $Q^4(nAl)$ distribution in the Alban Hills leucite-derived series, the widths and shapes of the spectra,
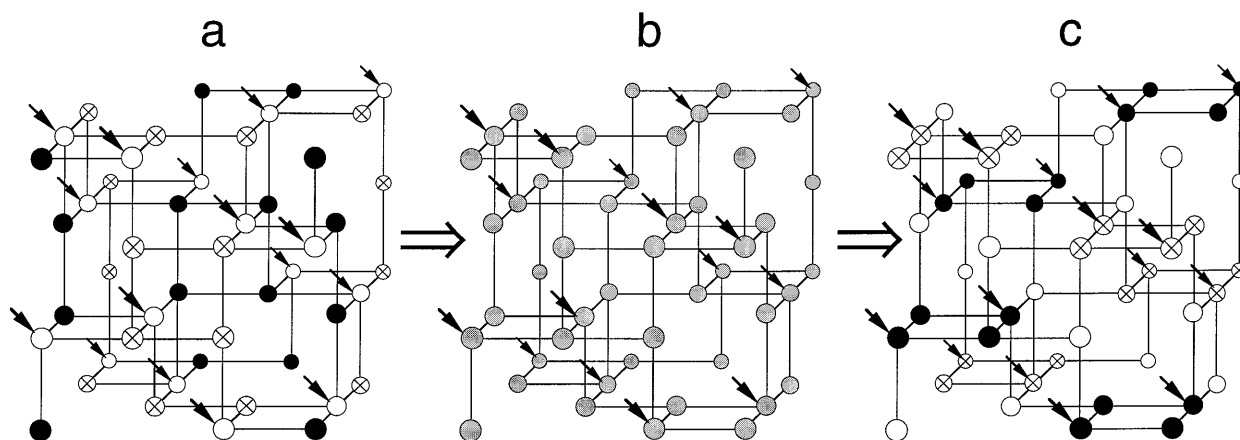
FIGURE 3. Schematic drawing showing how the T-site ordering can change during the ion-exchange process without diffusion of Al or Si. Filled circles = T1; open circles = T2; crossed circles = T3. The arrows indicate the positions occupied by Al. (**a**) Starting configuration in tetragonal phase with Al ordered entirely onto T2 site. The T1, T2, and T3 configuration is the same as that shown by Murdoch et al. (1988). (**b**) Cubic phase with all T sites symmetrically equivalent, but Al in same positions. (**c**) Final product of ion exchange in tetragonal phase below T_c. T sites have changed, but Al and Si are on the same positions as **a**. Note that the T1, T2, and T3 connectivities in 3a and 3c are identical.

especially for the K and Rb members of the series, suggest strongly that only small differences exist in the $Q^4(n\text{Al})$ distributions. These relationships indicate that Si and Al atoms do not exchange positions within the framework to any significant degree during the ion-exchange process, consistent with the large literature on ion exchange in feldspars (e.g., Kroll et al. 1986).

In contrast to the small changes in the Al NNN distribution within each series, there are large changes in the long-range ordering of Al and Si over the three T sites. In the analcite-derived series, the Al partitioning over the T sites changes from approximately 50% on T2 (KAlSi_2O_6 leucite) to 20% on T2 ($\text{RbAlSi}_2\text{O}_6$ leucite) to 70% on T2 ($\text{CsAlSi}_2\text{O}_6$ leucite). We stress that the large changes in T-site ordering do not depend on complex fitting procedures; the differences between these estimates of the long range Si-Al order are much larger than the errors involved. Even a simple visual inspection of the spectra (Fig. 1) confirms the large differences in T-site occupancies between the three analcite-derived samples. The changes are particularly clear in the ^{27}Al spectra where there is only one peak for each T site (because of Al avoidance). The changes in long-range Si-Al order in the Alban Hills leucite are difficult to quantify because of the wider $Q^4(n\text{Al})$ distribution in this series. It is therefore impossible to establish whether the trends are the same as those observed in the analcite-derived series.

The changes in T-site ordering are not easy to explain, because we have already seen that Si and Al appear to be nearly fixed within the framework during ion exchange. The only way that these two observations can be reconciled is to suggest that a conformational change of the structure occurs in such a way that a particular site changes its character from being, for example, a T2 site before the ion exchange to a T3 site after. We suggest

that this is possible if the ion exchange is performed above the tetragonal-cubic phase transition temperature of the leucite, where all the T sites are symmetrically equivalent. To clarify this point, consider a hypothetical example in which all Al is on T2 and all Si is on T1 and T3 (Fig. 3a). Above T_c, all the sites are symmetrically equivalent, but if the Si and Al do not exchange, all the Al still have four Si NNN and all the Si still have two Al NNN (Fig. 3b). When the sample is cooled below T_c, it has no memory of which T sites were originally T1, T2, or T3, and distortion of the framework can occur to give the most energetically favorable conformation. Thus it is possible that a sample could be produced in which the Al is split between T1 and T3, with all Al having four Si NNN as before, and with Si occupying all T2 sites and one-half of the T1 and T3 sites, again with all the Si having two Al NNN (Fig. 3c). Note that although the absolute positions of the T1, T2, and T3 labels have changed between Figures 3a and 3c, their relative positions and the characteristic leucite structure connectivities (T1 linked to two T1 and two T2, T2 linked to two T1 and two T3, T3 linked to two T3 and two T2) are unchanged. Note also that in Figure 3a the four membered-rings containing four T1 and four T3 are in the plane of the paper, whereas in Figure 3b these rings are perpendicular to the plane of the paper, i.e., the orientation of the c axis has changed. There is a third possible orientation (not illustrated) where such four-membered rings are perpendicular to both the planes illustrated in Figure 3.

An additional example is shown in Figure 4, which has the same T1, T2, and T3 arrangements as Figure 3, but with Si and Al distributed differently over the T sites. In Figure 4a, five Al atoms are on T1, five Al are on T2, and six Al are on T3. In Figure 4c, again without exchanging any Si with Al, the Al occupancies on T1, T2,
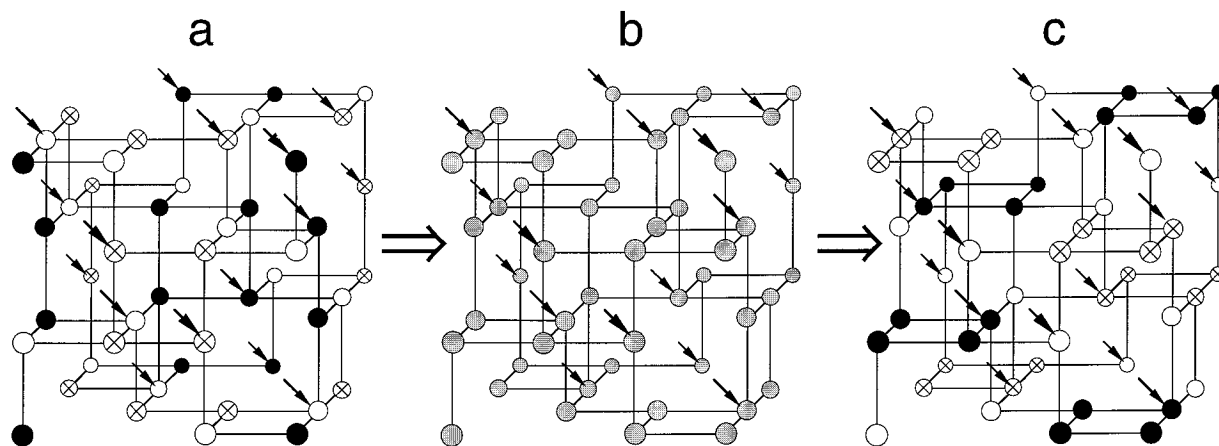
Figure 4. Extension of the model proposed in Figure 3, but with a more complex T-site ordering scheme in the starting material. Filled circles = T1; open circles = T2; crossed circles = T3. The arrows indicate the positions occupied by Al. (**a**) tetragonal phase; (**b**) cubic phase; (**c**) tetragonal phase after ion exchange.

and T3 are 4:8:4. Furthermore, large changes occur in the $Q^4(n\text{Al})$ distribution (short-range order) for each T-site type, though obviously the sum of the $Q^4(n\text{Al})$ distributions over all three T-site types remains the same in Figures 4a and 4c. Clearly, wide ranges of T-site ordering are possible, all of which maintain the correct connectivities. The conclusion from Figures 3 and 4 is that a wide range of long-range (T-site) order can be generated with exactly the same local order and it follows that T-site order has little influence on the thermodymanic properties of leucite.

It seems likely that the orientation of collapse of the aluminosilicate framework is coupled to the geometry of the W site, giving rise to the very different T-site ordering patterns observed for the K, Rb, and Cs samples. The properties of the alkali cation in the W site (size, charge, polarizability, and so forth) therefore control the final T-site ordering. In this context, note that Palmer et al. (1997) have shown recently that the cubic phase of $RbAlSi_2O_6$ has a larger tetrahedral distortion (i.e., larger T-O bond length variations) than either $KAlSi_2O_6$ or $CsAlSi_2O_6$. It is therefore tempting to speculate that the very different ordering of Al in the Rb member of the analcite-derived series in comparison with the K and Cs members is related somehow to the local framework geometry in the cubic phase prior to the cubic-tetragonal transition.

To summarize, our data suggest that the identity of the cation in the W site affects the orientation of the framework distortions associated with the cubic-tetragonal phase transition and leads to the possibility that a particular tetrahedral cation site can take on the characteristics of a T1, T2, or T3 site. In a sample with complete Si-Al disorder this effect would not be detectable; however, in samples with partially (or completely) ordered Si-Al arrangements, completely different Al-ordering patterns on T1, T2, and T3 are possible, leading to different relative

intensities of T1, T2, and T3 peaks in ^{29}Si and ^{27}Al spectra.

Correlation of NMR chemical shift with structure

The analcite-derived series with their highly ordered Al NNN distributions provide an excellent opportunity to study correlations between ^{29}Si NMR chemical shifts for $Q^4(2\text{Al})$ Si and structural parameters. Figure 5 shows the correlations between the ^{29}Si chemical shift and both the mean T-O-T angle and mean T-T distance of $Q^4(2\text{Al})$ Si. The data sources are listed in the figure caption. It should be noted that the structural data of Palmer et al. (1997) were obtained for a natural leucite as well as ion-exchanged leucite samples derived from a natural leucite, therefore it could be argued that the T-O-T angles and T-T distances in the analcite-derived samples might be different. However, comparison of the ^{29}Si peak positions in ordered and disordered $KAlSi_2O_6$ leucite (Kohn et al. 1995) suggest that this is not the case and that the ^{29}Si shifts are not significantly different in both samples. Note that although we have not performed fits of the Rb or Cs samples derived from Alban Hills leucite it appears likely that the $Q^4(2\text{Al})$ peaks for each of the three sites are at the same shift for both series of samples.

Figure 5 shows the excellent correlation between the ^{29}Si chemical shift and the mean T-O-T angle for all sites in the three leucite samples and for analcite. The four data points for wairakite define a parallel or sub-parallel trend displaced by about 3 ppm. The discrepancy for wairakite probably relates to the replacement of the univalent Na^+ cation with a divalent Ca^{2+} cation. This results in vacant cavity sites and, crucially, a much stronger interaction between the framework and Ca than any of the other cations (shown by the anomalously short Ca-O bond lengths). The T-T distance correlation is also excellent, with a gradient of -94.2 ppm/Å, in comparison with -145.1 ppm/Å for tridymite (Kitchin et al. 1996).
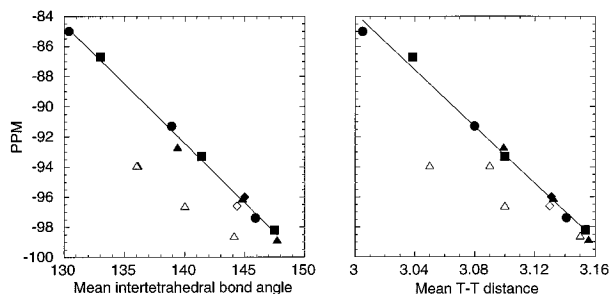
FIGURE 5. The ^{29}Si chemical shifts of Q^4(2Al) Si atoms in leucite and leucite-related compounds, plotted as a function of the mean intertetrahedral angles (T-O-T) (in degrees) and mean T-T distances (in angstroms). All the filled symbols are leucite compounds; circles = KAlSi$_2$O$_6$; squares = RbAlSi$_2$O$_6$; triangles = CsAlSi$_2$O$_6$; diamond = cubic CsAlSi$_2$O$_6$ at 150 °C. Open diamond is analcite and open triangles are wairakite. The data sources used are Kohn et al. 1995 (NMR data for analcite, analcite-derived KAlSi$_2$O$_6$ leucite), Henderson et al. 1997 (NMR and structural data for wairakite), Phillips and Kirkpatrick 1994 (NMR data for cubic CsAlSi$_2$O$_6$), this work (NMR data for analcite-derived RbAlSi$_2$O$_6$ and CsAlSi$_2$O$_6$ leucite compounds), Mazzi and Galli 1978 (structural data for analcite), and Palmer et al. 1997 (structural data for all leucite compounds). The solid lines are the best fits including only the K, Rb, and Cs samples, with the equations δ = 18.18 − 0.790 ⟨T-O-T⟩ and δ = 198.77 − 94.19 ⟨T-T⟩.
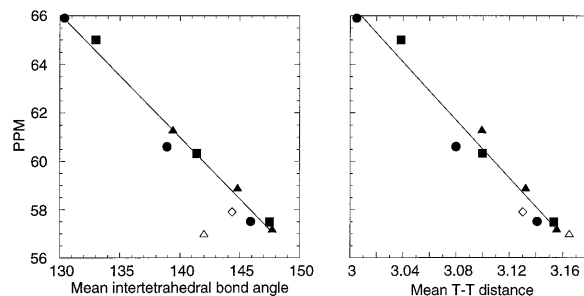
FIGURE 6. The ^{27}Al shifts of Al in leucite and leucite-related compounds, plotted as a function of the mean intertetrahedral angles (T-O-T) (in degrees) and mean T-T distances (in angstroms). All the filled symbols are leucite compounds; circles = KAlSi$_2$O$_6$; squares = RbAlSi$_2$O$_6$; triangles = CsAlSi$_2$O$_6$. Open diamond is analcite and open triangle is wairakite. ^{27}Al data from this study and Kohn et al. (1995), except wairakite from Henderson et al. (1997); structural data from Palmer et al. (1997) (KAlSi$_2$O$_6$, RbAlSi$_2$O$_6$, and CsAlSi$_2$O$_6$), Mazzi and Galli (1978) (analcite), and Henderson et al. (1997) (wairakite). All shifts are peak positions at 14.1 T, except wairakite, which is isotropic chemical shift obtained by simulation of MAS line shapes. The solid lines are the best fits including only the K, Rb, and Cs samples with the equations δ = 132.24 − 0.509 ⟨T-O-T⟩ and δ = 246.39 − 59.965 ⟨T-T⟩

Figure 6 shows the correlations between the ^{27}Al chemical shift and both the mean T-O-T angle and mean T-T distance. Since the ^{27}Al spectra were obtained at 14.1 T, and the lines are fairly narrow, the contribution of the quadrupolar shift to the peak position is likely to be small (and similar for all the lines). Thus the peak maxima are a reasonable approximation to the isotropic chemical shift. The exception is the ^{27}Al resonances for wairakite (Henderson et al. 1997) for which the isotropic shift (estimated from simulations) is used. The angle correlation can be compared with those of Lippmaa et al. (1986), Phillips et al. (1989), and Phillips and Kirkpatrick (1994). We find δ = 132.2 − 0.509 ⟨T-O-T⟩, which is very similar to the correlations found by Phillips et al. (1989) and Phillips and Kirkpatrick (1994) for leucite and Lippmaa et al. (1986) for disordered silicates. The difference between our data and those of Phillips et al. (1989) and Phillips and Kirkpatrick (1994) over the range of angles in leucite is that our shifts are 2–3 ppm more negative, largely because we are reporting center band peak positions at high field whereas Phillips et al. (1989) and Phillips and Kirkpatrick (1994) estimated the isotropic chemical shift from the spinning sidebands of the satellite transitions. Again note that the wairakite point falls off the trend toward lower mean T-O-T angles (cf. Fig. 5).

REFERENCES CITED

Baltisberger, J.H., Xu, Z., Stebbins, J.F., Wang, S.H., and Pines, A. (1996) Triple-quantum 2-dimensional ^{27}Al magic angle spinning nuclear magnetic resonance spectroscopic study of aluminosilicate and aluminate crystals and glasses. Journal of the American Chemical Society, 118, 7209–7214.

Bell, A.M.T and Henderson, C.M.B. (1994) Rietveld refinement of the structures of dry-synthesized MFe^{3+}Si$_2$O$_6$ leucites (M = K, Rb, Cs) by synchrotron x-ray-powder diffraction. Acta Crystallographica, C50, 1531–1536.

——— (1996) Rietveld refinement of the orthorhombic *Pbca* structures of Rb$_2$CdSi$_5$O$_{12}$, Cs$_2$MnSi$_5$O$_{12}$, Cs$_2$CoSi$_5$O$_{12}$ and Cs$_2$NiSi$_5$O$_{12}$ leucites by synchrotron x-ray-powder diffraction. Acta Crystallographica, C52, 2132–2139.

Bell, A.M.T., Henderson, C.M.B., Redfern, S.A.T., Cernik, R.J., Champness, P.E., Fitch, A.N. and Kohn, S.C. (1994a) Structure of synthetic K$_2$MgSi$_5$O$_{12}$-leucites by integrated X-ray powder diffraction, electron diffraction and ^{29}Si MAS NMR methods. Acta Crystallographica, B50, 31–41.

Bell, A.M.T, Redfern, S.A.T., Henderson, C.M.B., and Kohn, S.C. (1994b) Structural relations and tetrahedral ordering pattern of synthetic orthorhombic Cs$_2$CdSi$_5$O$_{12}$ leucite: an integrated synchrotron X-ray powder diffraction and ^{29}Si MAS NMR study. Acta Crystallographica, B50, 560–566.

Brown, I.W.M., Cardile, C.M., MacKenzie, K.J.D., Ryan, M.J., and Meinhold, R.H. (1987) Natural and synthetic leucites studied by solid state 29-Si and 27-Al NMR and 57-Fe Mössbauer spectroscopy. Physics and Chemistry of Minerals, 15, 78–83.

Hatch, D.M., Ghose, S., and Stokes, H.T. (1990) Phase transitions in leucite, KAlSi$_2$O$_6$: I. Symmetry analysis with order parameter treatment and the resulting microscopic distortions. Physics and Chemistry of Minerals, 17, 220–227.

Henderson, C.M.B., Bell, A.M.T., Kohn, S.C., and Page, C.S. (1997) Leucite-pollucite structure type variability and the structure of a synthetic end-member calcium wairakite (CaAl$_2$Si$_4$O$_{12}$·2H$_2$O). Mineralogical Magazine, in press.

Ito, Y., Kuehner, S., and Ghose, S. (1991) Phase transitions in leucite determined by high temperature single crystal X-ray diffraction. Zeitschrift für Kristallographie, 197, 75–84.

Kitchin, S.J., Kohn, S.C., Dupree, R., Henderson, C.M.B., and Kihara, K. (1996) In situ ^{29}Si MAS NMR studies of structural phase transitions of tridymite. American Mineralogist, 81, 550–560.

Kohn, S.C., Henderson, C.M.B., Mortuza, M.G., and Dupree, R. (1991) An NMR study of structure and ordering in synthetic $K_2MgSi_5O_{12}$, a leucite analogue. Physics and Chemistry of Minerals, 18, 144–154

Kohn, S.C., Henderson, C.M.B. and Dupree, R. (1994) NMR studies of the leucite analogues $X_2YSi_5O_{12}$, where X = K, Rb, Cs Y = Mg, Zn, Cd. Physics and Chemistry of Minerals, 21, 176–190.

——— (1995) Si-Al order in leucite revisited: New information from an analcite-derived analogue. American Mineralogist, 80, 705–714.

Kroll, H., Schmiemann, I., and von Cölln, G. (1986) Feldspar solid solutions. American Mineralogist, 71, 1–6.

Lange, R.A., Carmichael, I.S.E., and Stebbins, J.F. (1986) Phase transitions in leucite ($KAlSi_2O_6$), orthorhombic $KAlSiO_4$, and their iron analogues ($KFeSi_2O_6$, $KFeSiO_4$). American Mineralogist, 71, 937–945.

Lippmaa, E., Samoson, A., and Mägi, M. (1986) High-resolution ^{27}Al NMR of aluminosilicates. Journal of the American Chemical Society, 108, 1730–1735.

Mazzi, F. and Galli, E. (1978) Is each analcime different? American Mineralogist, 63, 448–460.

Murdoch, J.B., Stebbins, J.F., Carmichael, I.S.E., and Pines, A. (1988) A silicon-29 nuclear magnetic resonance study of silicon ordering in leucite and analcite. Physics and Chemistry of Minerals, 15, 370–382.

Palmer, D.C., Dove, M.T., Ibberson, R.M., and Powell, B.M. (1997) Structural behavior, crystal chemistry, and phase transitions in substituted leucite: High-resolution neutron powder diffraction studies. American Mineralogist, 82, 16–29.

Phillips, B.L. and Kirkpatrick, R.J. (1994) Short-range Si-Al order in leucite and analcime: Determination of the configurational entropy from ^{27}Al and variable temperature ^{29}Si NMR spectroscopy of leucite, its Cs- and Rb-exchanged derivatives, and analcime. American Mineralogist, 79, 1025–1031.

Phillips, B.L., Kirkpatrick, R.J., and Putnis, A. (1989) Si,Al ordering in leucite by high-resolution ^{27}Al MAS NMR spectroscopy. Physics and Chemistry of Minerals, 16, 591–598.

Taylor, D. and Henderson, C.M.B. (1968) The thermal expansion of the leucite group of minerals. American Mineralogist, 53, 1476–1489.